THE ENERGY BALANCE IN THE POSITIVE COLUMN OF A LONGITUDINAL GAS DISCHARGE AT ATMOSPHERIC PRESSURE

P. I. Porshnev

UDC 537.525

A two-dimensional positive-column model is described that includes the major features of a low-temperature nitrogen plasma. Ionization mechanisms for nitrogen in an atmospheric-pressure discharge are examined.

Research on gas discharges is important because they are widely used in quantum electronics, plasma chemistry, and various engineering processes. It is important to determine how the external conditions govern the internal parameters such as the translational and vibrational temperatures, field strength, and electron concentration. A detailed simulation has been performed [1] for a nitrogen plasma on the basis of vibrational relaxation and stepwise and associative ionization, but it was one-dimensional and did not incorporate the spatial distributions in the parameters, which are particularly important for high energy deposition, when the gas temperature greatly exceeds the wall temperature. The two-dimensional current flow in a longitudinal discharge has been incorporated [2]. The equations for the electron concentration have been written in the ambipolar diffusion apporoximation in [2] and differ substantially from the form in [3, 4], which probably means that they are incorrect, since the convective term in [2] includes the electron drift velocity, not the hydrodynamic flow speed (see also [5]).

Here I present a two-dimensional model for a longitudinal discharge that incorporates the major kinetic features for a nitrogen plasma. The basis is the joint solution of the two-dimensional equations for thermal conduction, the boundary layer, and the electron concentration, together with the equations for the vibrational kinetics in the anharmonic approximation, Boltzmann's equation for the electronic levels in nitrogen. The model differs essentially from [1, 2] in that it incorporates the Boltzmann equation for the energy distribution, which enables one to incorporate collisions of the second kind with vibrationally and electronically excited molecules. The vibrationally excited states affect the properties of a nitrogen plasma [6, 7]; studies have been made [8] on how electronically excited levels affect the direct ionization rate for nitrogen. Here I show that incorporating collisions of the second kind with those molecules substantially increases the associative ionization rate and produces corresponding changes in the voltage-current characteristics.

Consider a stationary longitudinal discharge in a cylinder, with the cathode upstream. The charged-particle distribution in a weakly ionized plasma that meets the quasineutrality condition is found from the electron-balance equation in the ambipolar-diffusion approximation [3]:

$$\rho u \frac{\partial}{\partial z}\frac{n_e}{\rho} + \rho v \frac{\partial}{\partial r}\frac{n_e}{\rho} = \frac{1}{r}\frac{\partial}{\partial r}\left(D_a \rho r \frac{\partial}{\partial r}\frac{n_e}{\rho}\right) + k_i N n_e - \beta n_e^2 + S_i;$$

$$n_e|_{r=R} = 0; \quad \left.\frac{\partial n_e}{\partial r}\right|_{r=0} = 0; \quad n_e|_{z=0} = n_e^0(r). \tag{1}$$

At atmospheric pressure, the ion composition in a nitrogen plasma is governed by N_4^+ particles, so we take the electron-ion recombination coefficient as $\beta = 10^{-7}$ cm^3/sec with $D_a\rho = (\mu_+\rho)T_e = 2.6\cdot 10^{-4}\ T_e$ kg/m·sec. The direct-ionization rate constant $k_i(E/N)$ and T_e are calculated by averaging the electron-energy distribution over the discharge-electron spectrum. The source S_i describes the electron generation in stepwise and associative ionization of

Lykov Institute for Heat and Mass Transfer, Belorussian Academy of Sciences, Minsk.
Translated from Inzhenerno-Fizicheskii Zhurnal, Vol. 58, No. 5, pp. 814-820, May, 1990. Original article submitted February 21, 1989.

0022-0841/90/5805-0631$12.50

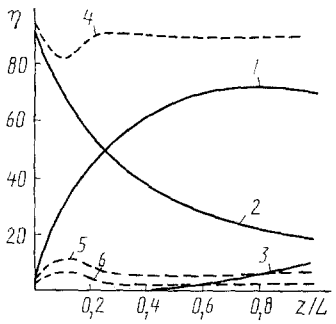

Fig. 1. Current energy distribution (I = 25 mA, G = 0.05 g/sec, R = 0.2 cm, L = 3 cm): 1) gas heating; 2 and 4) vibrational excitation; 3) heat loss to wall; 5) electronic-level excitation; 6) direct gas heating by electrons η, %.

metastable levels in the nitrogen molecule. Ambipolar drift is not incorporated in (1) [5], and it is proposed to consider the effects on the positive-column characteristics in a separate paper.

The electric field E is found from the condition for constancy of the total current I along the tube: $I = 2\pi \int_0^R en_e \mu_e E r dr$.

The hydrodynamic flow speed is determined from the equations of two-dimensional gas dynamics in the boundary-layer approximation:

$$\rho u \frac{\partial u}{\partial z} + \rho v \frac{\partial u}{\partial r} = \frac{1}{r} \frac{\partial}{\partial r} \left(\mu(T) r \frac{\partial u}{\partial r} \right) - \frac{dp}{dz}, \tag{2}$$

$$u|_{r=R} = 0; \quad \left. \frac{\partial u}{\partial r} \right|_{r=0} = 0; \quad u|_{z=0} = u^0(r);$$

$$\frac{\partial}{\partial z} \rho u r + \frac{\partial}{\partial r} \rho v r = 0. \tag{3}$$

The unknown pressure gradient is derived from the condition for constant mass flow rate $G = 2\pi \int_0^R \rho u r dr$.

The thermal-conduction equation with radiative transport neglected is put as

$$u \rho c_p \frac{\partial T}{\partial z} + \rho v c_p \frac{\partial T}{\partial r} = \frac{1}{r} \frac{\partial}{\partial r} \left(\lambda(T) r \frac{\partial T}{\partial r} \right) + Q_e + Q_{vib} + Q_m, \tag{4}$$

$$T|_{r=R} = T_{ст}; \quad \left. \frac{\partial T}{\partial r} \right|_{r=0} = 0; \quad T|_{z=0} = T^0(r).$$

The sources Q_{vib} and Q_m express the heating correspondingly in vibrational relaxation and metastable-level quenching, while Q_e is the proportion of the current energy going directly to produce heat by elastic collisions between electrons and nitrogen molecules. The [9] temperature dependence was used for the viscosity and thermal conductivity.

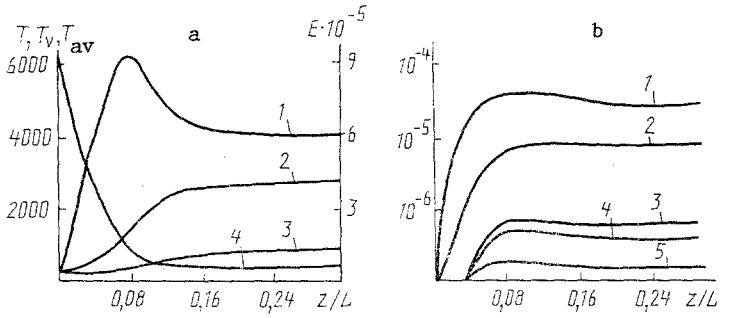

Fig. 2. Dependence of discharge parameters on longitudinal coordinate (I = 25 mA, G = 0.05 g/sec, R = 0.2 cm, L = 3 cm): a) 1) T_V (at axis); 2) T (at axis); 3) T_{av}; 4) E; b) relative particle concentrations at axis: 1) $N_2(A^3\Sigma_u^+)$, 2) $N_2(a'^1\Sigma_u^-)$, 3) n_e, 4) $N_2(B^3\Pi_g)$, 5) $N_2(C^3\Pi_u)$.

The electron energy distribution is derived from Boltzmann's equation [10]:

$$\frac{1}{3}\left(\frac{E}{N}\right)^2 \frac{d}{d\varepsilon}\left(\frac{\varepsilon}{Q_m}\frac{df}{d\varepsilon}\right) + 2\frac{m}{M}\frac{d}{d\varepsilon}\left(\varepsilon^2 Q_M f + \frac{kT}{e}\frac{df}{d\varepsilon}\right) = \sum_j [(\varepsilon+\varepsilon_j)\,Q_j(\varepsilon+\varepsilon_j)\,f(\varepsilon+\varepsilon_j)\,N_j - \varepsilon Q_j(\varepsilon) f(\varepsilon) N_j + (\varepsilon-\varepsilon_j)\,Q_j^*(\varepsilon-\varepsilon_j) f(\varepsilon-\varepsilon_j) N_j^* - \varepsilon Q_j^*(\varepsilon) f(\varepsilon) N_j^*]. \quad (5)$$

The electron-N_2 interaction cross sections needed to solve (5) were taken from [11]. The distribution satisfies the normalization condition $\int_0^\infty f(\varepsilon)\varepsilon^{1/2}d\varepsilon = 1$, and then the electron mobility and temperature are given by

$$\mu_e = -\frac{1}{3N}\left(2\frac{e}{m}\right)^{1/2}\int_0^\infty \varepsilon Q_M(\varepsilon)\frac{df}{d\varepsilon}d\varepsilon, \quad T_e = \frac{2}{3}\int_0^\infty \varepsilon^{3/2} f(\varepsilon)\,d\varepsilon.$$

The (5) distribution enables one to determine also the constants for the forward and reverse inelastic processes:

$$k_j = \left(2\frac{e}{m}\right)^{1/2}\int_0^\infty \varepsilon Q_j(\varepsilon) f(\varepsilon)\,d\varepsilon, \quad (6)$$

$$k_j^* = \left(2\frac{e}{m}\right)^{1/2}\int_0^\infty \varepsilon Q_j(\varepsilon) f(\varepsilon-\varepsilon_j)\,d\varepsilon. \quad (7)$$

Here (5) contains N_j^*, the relative populations in the excited molecular-nitrogen levels. Those levels here were takn as vibrational ones having v = 1-8 in the $X^1\Sigma_g^-$ ground state and in the $A^3\Sigma_u^+$, $B^3\Pi_g$, $C^3\Pi_u$, $a'^1\Sigma_u^-$ electronic levels. We incorporated the effects of the populations in those states on major characteristics via collisions of the second kind, whose incorporation usually increased the constants for the direct and stepwise ionization.

The distribution over the vibrational levels in the ground electronic state was derived from the vibrational-kinetics equations in the anharmonic approximation [6]:

$$\rho u \frac{d}{dz}\frac{f_v}{\rho} = \Pi_v^{VV} + \Pi_v^{VT} + k_v N n_e - k_v^* n_e f_v. \quad (8)$$

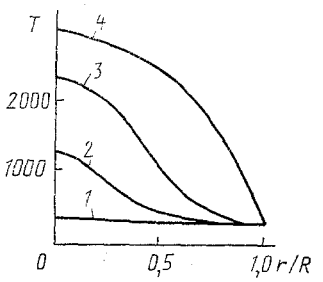

Fig. 3

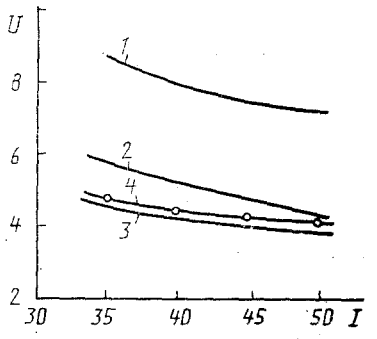

Fig. 4

Fig. 3. Radial translational-temperature profiles (I = 25 mA, G = 0.05 g/sec, R = 0.2 cm, L = 3 cm): 1) z/L = 0; 2) 0.07; 3) 0.12; 4) 1. T, K.

Fig. 4. Voltage–current characteristics (G = 0.12 g/sec, R = 0.1 cm, L = 3 cm): 1) direct ionization; 2 and 3) associative ionization; 4) experiment [17]. U in kV and I in mA.

The terms Π_v^{VV} and $\Pi_v^{V\tau}$, which reflect the contributions from V-V and V-T processes, have been expressed in more detail in [6]; the constants for those processes were taken from [12]. We calculated the populations of 30 vibrational levels, which is a number sufficient to describe the stored vibrational energy satisfactorily. Consequently, we did not consider associative ionization arising from collisions with vibrationally excited nitrogen molecules.

The electronic-level populations were described from the kinetic schme

$$N_2(A) + N_2(A) = N_2(B) + N_2(X), \quad e^- + N_2(X) = e^- + N_2(A),$$
$$N_2(A) + N_2(A) = N_2(C) + N_2(X), \quad e^- + N_2(X) = e^- + N_2(B),$$
$$N_2(A) + N_2(X) = N_2(X) + N_2(X), \quad e^- + N_2(X) = e^- + N_2(C),$$
$$N_2(A) + N_2(X) = N_2(B) + N_2(X), \quad e^- + N_2(X) = e^- + e^- + N_2^+,$$
$$N_2(B) + N_2(X) = N_2(X) + N_2(X), \quad e^- + N_2(A) = e^- + e^- + N_2^+,$$
$$N_2(C) = N_2(B) + h\nu(2^+), \quad N_2(B) = N_2(A) + h\nu(1^+).$$

It has been suggested [2, 13] that associative ionization for the excited molecules in the $a'^1\Sigma_u^-$ state is important:

$$N_2(a') + N_2(a') = N_4^+ + e^-, \quad N_2(a') + N_2(A) = N_4^+ + e^-.$$

To incorporate this, we add the following reactions:

$$e^- + N_2(X) = e^- + N_2(a'), \; N_2(a') + N_2(a') = 2N_2(X), \; N_2(a') = N_2(X) + h\nu.$$

The rate constants for processes involving electrons were derived from (6) and (7), while for the other reactions, they were taken from [2, 14, 15].

The inlet gas temperature was taken as equal to the wall temperature (constant), while the electron concentration and gas flow speed were based on an initial parabolic profile.

System (1)-(8) and the kinetic equations for the electronic levels were solved by the [16] method. At each step, the iteration was condinued until the field and pressure gradient met the conditions for constant total current and mass flow rate.

The (1)-(8) model gives the characteristics for a laminar flow over a wide range in conditions. At high pressures and currents (the glow discharge becomes an arc one), when the degree of ionization is $\geq 10^{-4}$ and the gas temperature exceeds 4000 K, the model becomes inapplicable because it does not incorporate electron-electron and electron-ion collisions or

radiative transport. At low pressure ($p \leq 1$ Tor), the applicability is limited by conditions that lead to a violation of the assumption that the energy distribution is local.

The basic form involves conditions characteristic of the [17] apparatus, which produced such a discharge. The solid lines in Fig. 1 show the integral energy balance normalized to IE, while the dashed lines show the specific energy balance (at the axis) normalized to jE. The latter is derived from (5) and the former by averaging the various energy fluxes over the cross section. Usually, $jE \geq 10^3$ W/cm^3 for an atmospheric-pressure discharge, and initially, most of the energy (about 90%) is deposited in the vibrational degrees of freedom, with only about 2% going directly to heating the gas. The vibrational temperature T_V (Fig. 2a) attains high values (≥ 6000 K), while the translational temperature T remains relatively low. There are many vibrationally excited molecules, which collide with the electrons and return part of the energy to them by collisions of the second kind, which raises the electron energy distribution in the region of the excitation thresholds for the electronic levels. The peak T_V in Fig. 2a is thus correlated with the positions of those maxima and with the minimum in the excitation of the vibrational levels in Fig. 1. Subsequently, the performance in exciting the electronic levels decreases because E/N falls, which is due to the fairly powerful ionization source.

The vibrational relaxation rate increases substantially at high T_V because of anharmonicity. The amount of energy released as heat during vibrational-translational relaxation becomes comparable with the pumping, and then energy is transferred from the electrons to heat via the molecular vibrational levels. The translational temperature rises to about 2500 K, and that redistribution means that most of the energy in the integral balance is consumed in heating the gas. As the temperature profile develops (Fig. 3), there is an increase in the proportion of the energy transmitted to the wall. The velocity profile remains almost parabolic, although the axial velocity roughly doubles. The pressure drop along the tube is slight and constitutes about 2% of the initial value.

E falls (Fig. 2a) because E/N decreases and T rises (as $p \cong$ const). Equations (5)-(7) show that E/N governs the excitation and ionization constants. The fall in E/N indicates an increase in ionization rate because numerous electronically excited molecules appear (Fig. 2b). Those molecules influence the ionization rate in two ways: firstly, $S_i = k(N_j^*)^2$, and secondly, by collisions of the second kind, which increase the excitation constants for the high-lying electronic levels and also by direct ionization. The last governs the ionization balance only at the start of the tube. Calculations on the voltage–current curves with allowance only for direct ionization give a result lying far bove the observed value (Fig. 4). Stepped ionization $N_2(A)$ has even less effect than direct, since the relative concentration of those particles does not exceed 10^{-4}.

Curves closest to experiment are obtained for associative ionization of molecules in the $a'^1\Sigma_u^-$ state (curves 2 and 3 in Fig. 4), but then it is important to correct for collisions of the second kind with electronically excited molecules. Published values exist for the quenching constants of the $A^3\Sigma_u^+$, $B^3\Pi_g$, $C^3\Pi_u$, $a'^1\Sigma_u^-$, states, so one can derive the populations in those states, so one can derive the populations in those states and correspondingly incorporate collisions of the second kind in (5). The quenching constants are unknown for the states $W^3\Delta_u$, $B'^3\Sigma_u^-$, $a^1\Pi_g$, $w^1\Delta_u$, and so on, and for them one is restricted to collisions of the first kind. Molecules excited to the $W^3\Delta_u$, and $B'^3\Sigma_u^-$, levels are assumed to pass by collision or radiation to the $B^3\Pi_g$, level, while $a^1\Pi_g$, $w^1\Delta_u$ one pass to $a'^1\Sigma_u^-$. The energy defect is correspondingly released as heat or radiated. It is purely symbolic to correct for that energy in the overall balance. The voltage–current curve calculated with associative ionization but without collisions of the second kind with electronically excited molecules is given by curve 2 in Fig. 4, while that with collisions of the second kind incorporated via the above mechanism is given in curve 3. All the calculated curves need to be displaced upwards by about 0.3 kV, which is the sum of the anode and cathode potential drops.

A simulation was performed with the two-dimensional conduction equations, the boundary layer, the electron concentration, the vibrational kinetics, and the electronics and electronic-level kinetics, which showed that in a longitudinal discharge at atmospheric pressure, most of the energy goes to heat the gas although initially the energy is deposited in the vibrational devrees of freedom. The main ionization mechanism is associative for molecules

in the $a'^1\Sigma_u^-$ state, but allowance must be made for collisions of the second kind with electronically excited molecules.

NOTATION

r and z, radial and axial coordinates; ρ and N, gas density and concentration; u and v, longitudinal and radial components of the gas pumping speed; n_e, electron concentration; D_a and β, ambipolar diffusion coefficient and dissociative electron recombination coefficient; k_j and k_j^*, forward and reverse rate constants for inelastic process j; S_i, associative ionization source; E, field strength; T_e, electron temperature; μ_+, mobility of N_4^+; e and m, electron charge and mass; R and L, tube radius and length; T and p, gas temperature and pressure; μ and λ, viscosity and thermal conductivity; G, mass flow rate; c_p, specific heat at constant pressure (without vibrational degrees of freedom); Q_{vib} and Q_m, energy deposited in vibrational relaxation and electronic-level quenching; Q_e, direct gas heating by electrons; T_w, wall temperature; T_v, vibrational temperature; T_{av}, average mass temperature; ε, electron energy; f, electron energy distribution; Q_M, cross section for elastic electron scattering at nitrogen molecules; Q_j and Q_j^*, cross sections for forward and reverse inelastic process j; M, molecular mass of nitrogen; k, Boltzmann's constant; ε_j, threshold for inelastic process j; N_j^*, populations of excited states of nitrogen molecule; μ_e, electron mobility; f_v, vibrational distribution; $N_2(X)$, $N_2(A)$, $N_2(B)$, $N_2(C)$, $N_2(a')$, nitrogen molecules in the states $X^1\Sigma_g^+$, $A^3\Sigma_u^+$, $B^3\Pi_g$, $C^3\Pi_u$, $a'^1\Sigma_u^-$; l; I discharge current; U, discharge burning voltage; j, current density.

LITERATURE CITED

1. Yu. S. Akishev, K. V. Baiadze, V. M. Vetsko, et al., Fiz. Plazmy, 11, No. 3, 999-1006 (1985).
2. H. Brunet and J. Rocca-Serra, J. Appl. Phys., 57, No. 5, 1574-1581 (1985).
3. Yu. P. Raizer, Gas-Discharge Physics [in Russian], Moscow (1987).
4. I. G. Galeev and B. A. Timirkaev, Teplofiz. Vys. Temp., 25, No. 5, 857-864 (1987).
5. F. I. Vysikailo and L. D. Tsendin, Fiz. Plazmy, 12, No. 10, 1206-1210 (1986).
6. J. Loureiro and C. M. Ferreira, J. Phys. B, 19, No. 1, 17-35 (1986).
7. N. L. Aleksandrov and I. V. Kochetov, Teplofiz. Vys. Temp., 25, No. 6, 1062-1067 (1987).
8. F. Paniccia, C. Gorse, J. Bretagne, and M. Capitelli, J. Appl. Phys., 59, No. 12, 4004-4006 (1986).
9. N. B. Vargaftik, Handbook on the Theromphysical Properties of Gases and Liquids [in Russian], Moscow (1972).
10. N. L. Aleksandrov, A. M. Konchakov, and É. E. Son, Fiz. Plazmy, 4, No. 1, 169-176 (1978).
11. N. L. Aleksandrov, F. I. Vysikailo, R. Sh. Islamov, et al., Teplofiz. Vys. Temp., 19, No. 1, 22-27 (1981).
12. G. D. Billing and E. R. Fisher, Chem. Phys., 43, No. 2, 395-401 (1979).
13. A. V. Berdyshev, I. V. Kochetov, and A. P. Napartovich, Fiz. Plazmy, 14, No. 6, 741-744 (1988).
14. D. I. Slovetskii, Reaction Mechanisms in Nonequilibrium Plasmas [in Russian], Moscow (1980).
15. L. G. Piper, J. Chem. Phys., 88, No. 1, 231-245 (1988).
16. S. V. Patankar and D. B. Spalding, Heat and Mass Transfer in Boundary Layers [Russian translation], Moscow (1971).
17. V. F. Kopylov, A. N. Ovcharenko, and A. I. Yaremenko, Physicochemical Processes in Nonequilibrium Plasmas [in Russian], Minsk (1985), pp. 42-44. (Coll., ITMO AN BSSR).